Conformational, Structural, and Chiroptical Properties of an Overcrowded Triply Fused Carbo[7]helicene

Albert Artigas, Nawal Ferdi, Maxime Rémond, Florian Rigoulet, Nicolas Vanthuyne, Denis Hagebaum-Reignier, Yannick Carissan, Jean-valère Naubron, Michel Giorgi, Ludovic Favereau, et al.

Conformational, structural and chiroptical properties of an overcrowded triply fused carbo[7]helicene

Albert Artigas,[a,†] Nawal Ferdi,[b] Maxime Rémond,[c] Florian Rigoulet,[a] Nicolas Vanthuyne,[a] Denis Hagebaum-Reignier,[a] Yannick Carissan,[a] Jean-Valère Naubron,[b] Michel Giorgi,[b] Ludovic Favereau,[c,*] Yoann Coquerel[a,*]

Author information

[a]Aix Marseille Université, CNRS, Centrale Méditerranée, ISM2, 13397 Marseille, France.

[b]Aix Marseille Université, CNRS, Centrale Méditerranée, FSCM, 13397 Marseille, France.

[c]Univ Rennes, CNRS, ISCR-UMR 6226, F-35000.

[†]Present address: Universitat de Girona, Facultat de Cieǹcies, Campus Montilivi, Carrer de Maria Aurelìa Capmanyi Farneś, 69, 17003 Girona, Catalunya, Spain.

E-mail:
ludovic.favereau@univ-rennes.fr
yoann.coquerel@univ-amu.fr

Graphical abstract

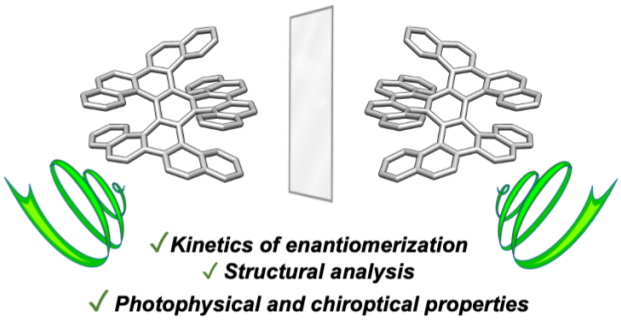

Abstract

Recently, the synthesis of the racemate of an overcrowded triply fused carbo[7]helicene of formula $C_{66}H_{36}$ with three carbo[7]helicene fused within a central six-membered ring was described. This molecule was found to embed an extremely contorted central six-membered rings and two negative curvatures. We report herein the resolution of the corresponding enantiomers and their conformational, structural, photophysical and chiroptical properties. The racemization of the triply fused carbo[7]helicene was determined to proceed at a rate $k_{rac} = 8.06 \cdot 10^{-4}$ s^{-1} at 175 °C in ortho-dichlorobenzene, corresponding to a barrier to enantiomerization $\Delta G_{enant}^{\ddagger} = 140.4$ kJ·mol^{-1}, a value significantly lower than for pristine carbo[7]Helicene. Interestingly, the crystalline structures of the racemic and enantiopure materials show some differences regarding the molecular geometry, with increased negative curvature in the latter cases. This unusual curved delocalized π-conjugated system afforded notably green fluorescence at room temperature and far-red phosphorescence at low temperature. Finally, electronic circular dichroism (ECD) and circularly polarized luminescence (CPL) responses of the enantiopure compounds have been measured and showed very close absorption and emission dissymmetry factors, g_{abs} and g_{lum}, respectively, of ca. $2.6 \cdot 10^{-3}$, indicating that the ground and excited states have similar chiral rigid geometries.

Introduction

Helicenes are defined as screw-shaped, inherently chiral, polycyclic aromatic molecules composed of ortho-fused aromatic rings. The handedness of the screw is noted either (*M*) or (*P*) for left-handed or right-handed helicenes, respectively. In their pristine form, carbo[*n*]helicenes are pure hydrocarbons made only of sp^2-hybridized C atoms spatially arranged in *n* ortho-fused six-membered rings (Figure 1).[1] The first report on the synthesis of carbo[5]helicene appeared as early as 1918, and the first successful synthesis of carbo[7]helicene was reported in 1967.[2] Since then and especially in the last two decades, the development of efficient synthetic approaches towards helicene and the related investigation of their photophysical and chiroptical properties have attracted significant attention. Indeed, the helical π-conjugated system provide them with rather intense chiroptical properties in comparison to other chiral molecules, which is of potential interest in a diverse range of applications going from chiroptoelectronics (organic light-emitting diodes [OLEDs], optical information processing, *etc.*) to bio-imaging and chiral sensing.[3] Molecular engineering around the helicene core (i.e.: size, heteroatoms/metal ions introductions, …) has become a topic of intense research to tune the resulting electronic and optical properties.[4] More recently, the design of more sophisticated chiral architectures, embedding several helical motifs, has become a new challenge in this topic of research, both from fundamental and potential applied aspects. These molecules, referred to as multiple helicenes or multihelicenes, embed several helical stereogenic elements and can thus exist, in principle, as diastereomers.[5] Because most multihelicenes are chiral in nature, and in the context of the development of small-molecule chirality in technological applications,[6] the determination and the rationalization of the chiroptical properties of symmetric multihelicenes has become a topic of considerable attention.[7]

The first example of a multihelicenes was reported by Erich Clar in 1959, with the synthesis of the double [5]helicene **D5H** (Figure 1).[8] It is only in 2007 that the conformational behavior of **D5H** was analyzed, using DFT methods, which revealed that **D5H** is a severely twisted molecule that can exist as two diastereomers: a chiral diastereomer of D_2-symmetry for which the enantiomers have the (*M,M*) or (*P,P*) configurations, and an achiral meso diastereomer of C_{2h} symmetry with the (*M,P*) configuration.[9] Comparison of the Gibbs free energies of both diastereomers revealed that the chiral diastereomer is the thermodynamic

diastereomer, stabilized by Δ(ΔG) = 21.5 kJ·mol^{-1} as computed at the b3lyp/6-31G(d) level of theory at 298 K. The enantiomerization process of the chiral diastereomer, from (*M,M*) to (*P,P*), was found to occur through the less stable meso diastereomer with a barrier to enantiomerization, also the barrier to diastereomers interconversion from (*M,M*) to (*M,P*) in this case, computed at $\Delta G_{enant}^{\ddagger} = \Delta G_{dia}^{\ddagger}$ = 132.6 kJ·mol^{-1} at the same level of theory. At the macroscopic scale, this indicates that the chiral diastereomer of **D5H** can exist as an enantiopure molecule at room temperature, but it was not verified experimentally. It can be noted that the enantiomerization barrier of D_2-**D5H** is significantly higher than the enantiomerization barrier of pristine carbo[5]helicene ($\Delta G_{enant}^{\ddagger}$ = 100.8 kJ·mol^{-1} at 300 K[10]). This probably results from the destabilization of the corresponding transition state because of the greater rigidity of the structure induced by the dibenzo[*cd*,*lm*]perylene core. Following Clar's pioneer work, some double [6]- and double [7]-helicenes were synthesized by Laarhoven[11] and Martin[12] in the early 1970's, and the field remained dormant for decades. It is at the dawn of the 21st century that the successful isolation of the first triple helicene could be confirmed, with the syntheses of both diastereomers of the triple [5]helicene **T5H**.[13] Despite the existence of three stereogenic elements in **T5H**, because of symmetry reasons, only two chiral diastereomers can exist: one diastereomer of D_3-symmetry embedding three helicene units of identical handedness for which the enantiomers have the (*M,M,M*) or (*P,P,P*) configurations, and one diastereomer of C_2-symmetry having one helicene unit with the opposite configuration of the two others for which the enantiomers have the (*P,M,M*) or (*M,P,P*) configurations (Figure 1). The stereochemical situation in **T5H** is comparable with the one in **D5H**. In fact, D_3-**T5H** was experimentally demonstrated the thermodynamic diastereomer, with a barrier to diastereomer interconversion from C_2-**T5H** to D_3-**T5H** in the magnitude of $\Delta G_{dia}^{\ddagger}$ = 109 kJ·mol^{-1} at 328 K (in d_2-tetrachloroethane).[13c] Revisiting this study, our own DFT calculations on the conformational behavior of **T5H**, performed at the ωB97XD/def2-TZVP//ωB97XD/def2-SVP level of theory (gas phase), confirmed i) that D_3-**T5H** is the thermodynamically favored diastereomer, by Δ(ΔG) = 18.6 kJ·mol^{-1} at 298 K, ii) that the calculated barrier to diastereomer interconversion from C_2-**T5H** to D_3-**T5H** is comparable with the measured one with $\Delta G_{dia}^{\ddagger}$ = 115.4 kJ·mol^{-1} at 328 K, and iii) that enantiomerization of D_3-**T5H** is occurring via the C_2-**T5H** diastereomer with a barrier computed at $\Delta G_{enant}^{\ddagger}$ = 133.5 kJ·mol^{-1} at 298 K (see details in the Supporting Information, Figure S1). Recently, the

two enantiomers of D_3-**T5H** could be resolved by chiral HPLC techniques and their chiroptical properties examined in detail,[14] but no experimental data is available on the kinetics of racemization of D_3-**T5H**. In 2017, Müllen, Narita and co-workers reported the synthesis of the chiral and meso diastereomers of the double [7]helicene **D7H**.[15] By analogy with **D5H**, D_2-**D7H** was determined the thermodynamic diastereomer with $\Delta(\Delta G) = 14.2$ kJ·mol^{-1} at the b3lyp/6-311G(d,p) level of theory (gas phase at 298 K). The barrier for the interconversion from D_2-**D7H** to C_{2h}-**D7H**, which is also the barrier to enantiomerization of D_2-**D7H**, was computed at $\Delta G_{dia}^{\ddagger} = \Delta G_{enant}^{\ddagger} = 192.5$ kJ·mol^{-1} at the same level of theory. The higher enantiomerization barrier of D_2-**D7H** compared to pristine carbo[7]helicene, for which $\Delta G_{enant}^{\ddagger} = 178.8$ kJ·mol^{-1} at 295 °C,[16] probably results from the destabilization of the corresponding transition state induced by the rigidity of the dibenzo[*cd*,*lm*]perylene core. The enantiomers of D_2-**D7H** were resolved by chiral HPLC techniques, which permitted the examination of some their chiroptical properties. Noteworthily, simultaneously with the report about **D7H**, the synthesis of another meso double [7]helicene having a different arrangement of the six-membered rings and C_i symmetry was reported by Bock, Durola and co-workers.[17]

In the past few years, the syntheses of several hexa-benzo and hexa-naphtho derivatives of molecule **T5H** have been reported, including diastereomers, and in some cases their chiroptical properties were examined when the resolution of the enantiomers could be achieved using chiral HPLC or the synthesis performed enantiospecifically from a single enantiomer of the substrate.[18] The common feature of all these molecules, is they embed three carbo[5]helicene units fused in a core six-membered ring, with the π-extension realized at the periphery. Notably, one of these molecules embeds the most twisted 'benzene' ring reported until now, with a maximum torsion angle measured at 36.9° (average of values measured in the racemate and both enantiopure monocrystalline solid states).[18d] Lately, our group has reported the successful synthesis of racemic C_2-**T7H**, a unique triple [7]helicene that embeds three carbo[7]helicene units fused in a core six-membered ring.[19] Racemic C_2-**T7H** was obtained efficiently through a nickel(0)-catalyzed [2 + 2 + 2] cycloaddition of 13,14-picyne, an aryne intermediate generated in situ. This overcrowded molecule is extremely contorted, with two accented negative curvatures and a severely distorted core six-membered ring showing a 36.5° maximum torsion angle in its

racemate monocrystalline solid state. The extreme contortion in C_2-**T7H** translated into an atypical aromaticity pattern, as analyzed by magnetic and electronic criteria of aromaticity. In the present article, we report the resolution of the enantiomers of C_2-**T7H** by chiral HPLC, the measurement of their rate of racemization, their structural parameters in the monocrystalline solid state, and their photophysical and chiroptical properties.

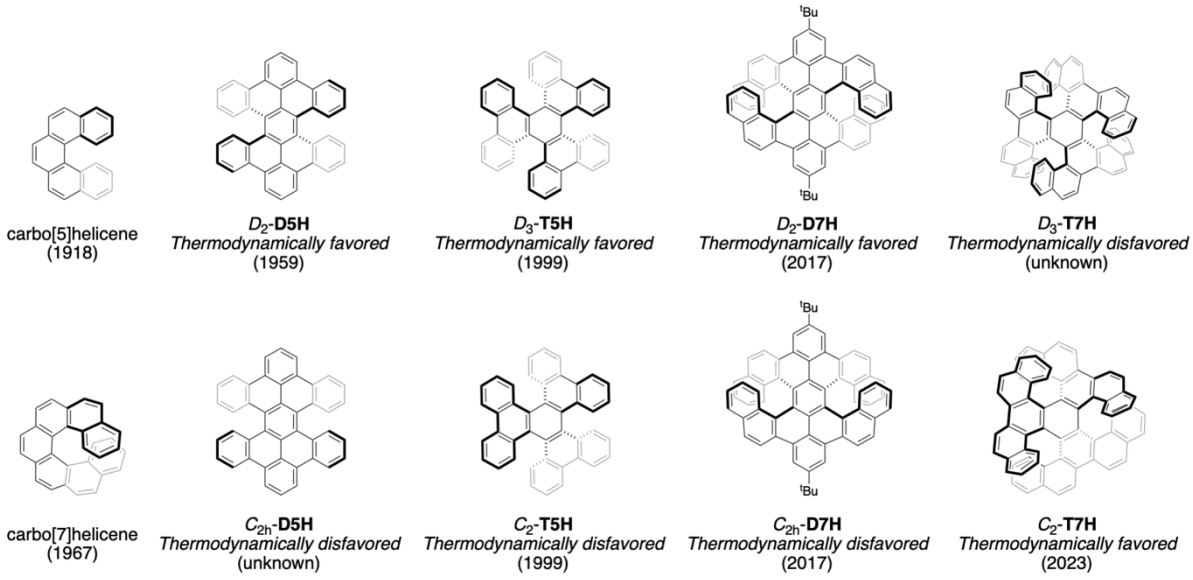

Figure 1. Selected examples of carbo[n]helicenes and multiple carbo[n]helicenes.

Results and discussion

In our previous work, examination of the conformational behavior of C_2-**T7H** in silico, using DFT methods at the ωB97XD/def2-TZVP//ωB97XD/def2-SVP level of theory, confirmed that only two chiral diastereomers can exist for this molecule.[19] By analogy with triple [5]helicene **T5H**, one diastereomer of **T7H** is of D_3-symmetry with three [7]helicene units of identical handedness for which the enantiomers have the (*M,M,M*) or (*P,P,P*) configurations, and the other diastereomer is of C_2-symmetry with one [7]helicene unit having the opposite configuration of the two others for which the enantiomers have the (*P,M,M*) or (*M,P,P*) configurations (Figure 1). However, in contrast with **T5H**, for **T7H**, the diastereomer with the lowest symmetry, that is C_2 vs D_3, is the thermodynamically favored diastereomer, with a $\Delta(\Delta G)$ = 25.8 kJ·mol^{-1} stabilization energy in favor of C_2-**T7H**. The preference for the C_2- over the D_3-symmetric diastereomer has previously been observed in comparable cases of overcrowded triphenylene derivatives.[20] The DFT study also revealed that the

enantiomerization of C_2-**T7H** is a single-step process, with a value of the barrier to enantiomerization computed at $\Delta G_{enant}^{\ddagger}$ = 150.1 kJ·mol^{-1} at 298 K, and that diastereomer interconversion from C_2-**T7H** to D_3-**T7H** is significantly more difficult with a barrier computed at $\Delta G_{dia}^{\ddagger}$ = 206.0 kJ·mol^{-1} at 298 K. These calculations indicate that diastereomer C_2-**T7H** cannot be thermally converted into diastereomer D_3-**T7H**, and that the actual value of the barrier to enantiomerization of C_2-**T7H** is experimentally accessible.

Separation of the two enantiomers of C_2-**T7H** was achieved by chiral preparative HPLC, which afforded samples with >99% enantiomeric excess (see details in Section S3 in the Supporting Information). The independent recrystallization of each enantiomer afforded single-crystals suitable for X-ray diffraction analysis, which permitted to assign their absolute configurations unambiguously (see Section S4 in the Supporting Information). Despite significant differences in the crystal packing of the racemate and the enantiopure forms, the asymmetric unit of C_2-**T7H** present very similar characteristics in all cases. The central ring exhibits the same severe twist angle of 36.5° in all forms. However, when considering the two negatively curved picene units, the negative curvature is significantly accentuated in the enantiopure form, with interplanar angles of the distal rings varying from 31.4–35.0° in the racemate to 31.5-41.5° in the enantiopure material (Figure 2, blue rings). The positively curved picene unit is also more twisted in the enantiopure material, with an interplanar angle varying from 7.7° in the racemate to 18.2° in the enantiopure material (Figure 2, blue rings). Consequently, the torsion at the core structure is reduced in the enantiopure material (see the green rings in Figure 2), with interplanar angles measured at 15.4° along the C_2 axis (vs 15.5° in the racemate) and 28.2-32.5° for the interplanar angles away from the C_2 axis (vs 33.8-34.1 in the racemate). These molecular geometric differences are most probably the consequence of different intermolecular interactions within the crystals. Indeed CH-π and π-π interactions are observed between solute molecules in the enantiopure materials while only inter-molecular π-π stackings are present between C_2-**T7H** moieties in the crystal of racemic C_2-**T7H** (see Section S4 in the Supporting Information). Moreover, racemic C_2-**T7H** co-crystallized with pentane (though too disordered to be localized)[19] while the enantiomeric forms co-crystallized with two molecules of chloroform, inducing C-H–π

interactions with the central and the peripheral cycles of the different picene units in the latter cases (see Figure S7 in the Supporting Information).

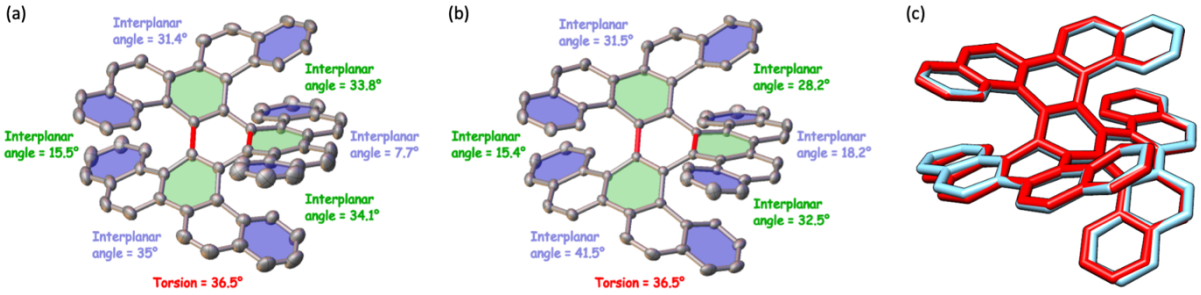

Figure 2. Some structural parameters for (*P,M,M*)-C_2-**T7H**: (a) in the racemate sample, adapted from reference 19, CCDC 2235879; (b) in the enantiopure sample, CCDC 2235878; (c) superposition of the racemate (red) and the enantiopure (cyan) materials. For the parameters of the (*M,P,P*)-C_2-**T7H** enantiomer, see CCDC 2235877.

The availability of enantiopure samples of both enantiomers of C_2-**T7H** allowed for the experimental determination of its racemization rate constant. This was realized by heating a ortho-dichlorobenzene solution of enantiopure (*M,P,P*)-C_2-**T7H** at exactly 175 °C, with an internal control of the temperature, and periodical monitoring of the enantiomeric excess by analytical HPLC (see details in the Supporting Information, section S5). Thus, the racemization of (*M,P,P*)-C_2-**T7H** was found to proceed at a rate $k_{rac} = 8.06 \cdot 10^{-4}$ s^{-1}, corresponding to a half-racemization life-time of 14.3 min and a barrier to enantiomerization $\Delta G_{enant}^{\ddagger} = 140.4$ kJ·mol^{-1} at 175 °C. Comparatively, the barrier to enantiomerization of C_2-**T7H** is significantly lower than of pristine carbo[7]helicene ($\Delta G_{enant}^{\ddagger} = 178.8$ kJ·mol^{-1} at 295 °C[16]). As previously observed for another symmetric multi-carbohelicene embedding three [7]helicene units,[18d] the primary factor responsible for this difference is certainly the destabilization of C_2-**T7H** induced by its extra crowding compared to pristine carbo[7]helicene. Adjusting the previously selected DFT level of theory to the experimental conditions, that is including a SMD solvation model for ortho-dichlorobenzene and thermodynamic corrections at 448 K, the barrier to enantiomerization of C_2-**T7H** was computed at $\Delta G_{enant}^{\ddagger} = 136.4$ kJ·mol^{-1} at 175 °C for C_2-**T7H** [DFT, ωB97XD/def2-TZVP(SMD=o-

dichlorobenzene,T=448 K)//ωB97XD/def2-SVP, see Section S2 in the Supporting Information]. This is less than 3% deviation from the experimentally determined value. The photophysical and chiroptical properties of the enantiomers of C_2-**T7H** were investigated in detail. The specific optical rotation of the enantiomers of C_2-**T7H** were determined in the magnitude of $|1{\cdot}10^3|$ at three different wavelengths (Table 1). Comparatively, the specific optical rotation of pristine [7]helicene is six times greater, with $[\alpha]_{579}^{25}$ = +5577 ($CHCl_3$, c = 0.01) for (*P*)-[7]helicene.[16]

λ (nm)	(*M,P,P*)-C_2-**T7H** $[\alpha]_\lambda^{25}$ (CH_2Cl_2, c = 0.025)	(*P,M,M*)-C_2-**T7H** $[\alpha]_\lambda^{25}$ (CH_2Cl_2, c = 0.030)
589	+ 940	- 935
578	+ 990	- 985
546	+ 1115	- 1110

Table 1. Specific optical rotations of the enantiomers of C_2-**T7H**.

The UV-vis absorption spectra of both enantiomeric samples were recorded in dichloromethane (Figure 3b, top). As expected, identical responses were obtained with a first transition at 220 nm ($\varepsilon \approx 80 \times 10^3$ M^{-1} cm^{-1}), followed by a more intense one at 285 nm ($\varepsilon \approx 100 \times 10^3$ M^{-1} cm^{-1}) with a shoulder around 315 nm, and a lower energy band with a maximum at 400 nm ($\varepsilon \approx 40 \times 10^3$ M^{-1} cm^{-1}) that extends to 475 nm. Electronic circular dichroism (ECD) measurements of enantiomers (*M,P,P*)-**T7H** and (*P,M,M*)-**T7H** resulted in perfect mirror-image spectra (Figure 3b, bottom), which for (*M,P,P*)-**T7H** includes one high-energy bisignate signal of positive and negative signs at 230 and 270 nm ($|\Delta\varepsilon| \approx 190$ M^{-1} cm^{-1}) respectively, a broader positive band at 350 nm ($\Delta\varepsilon \approx +180$ M^{-1} cm^{-1}), and two less intense negative peaks in the lower energy region, at 407 and 450 nm ($\Delta\varepsilon \approx -20$ M^{-1} cm^{-1}). The obtained signals at 270 and 350 nm for (*M,P,P*)-**T7H** are reminiscent of the characteristic ECD signature found for (*P*)-carbo[7]helicene regarding the ^1B_a and ^1B_b transitions,[21] albeit red-shifted by about 20 nm, reflecting the extended π-conjugated system for **T7H** in comparison to a more simple helicene unit. An absorption dissymmetry factor, g_{abs}, $2.6{\cdot}10^{-3}$ was determined at the first transition measured from the red-end (450 nm), which is one order of magnitude lower than the parent carbo[7]helicene compound (g_{abs} = $2.23{\cdot}10^{-2}$ at 350 nm),[21] but rather similar than more sophisticated multihelicene derivatives.[7] Although not vibronically resolved, the TD-DFT

calculations of the UV and ECD spectra of (*P,M,M*)-**T7H** are in very good agreement with the corresponding measured spectra and reproduce g_{abs} satisfactorily (see Section S6 in the Supporting Information). Comparison with the spectra calculated at the same level of theory for (*M*)-[7]helicene shows that the difference in g_{abs} results from both slightly lower average $\Delta\varepsilon$ values and significantly higher ε values for (*P,M,M*)-**T7H** compared to (*M*)-[7]helicene (see Section S6 in the Supporting Information). For both (*P,M,M*)-**T7H** and (*M*)-[7]helicene, the theoretical results clearly highlight the involvement of several transitions for the lowest energy excitation, which render complicated a direct analysis and comparison of the resulting electric and magnetic transition dipole moment vectors and their mutual angle. However, interesting information can be obtained by visual inspection of the frontier molecular orbitals (FMO) isosurface plots, which reveal that for **T7H** the electron density is localized mainly at the core, weakly involving the terminal rings of the [7]helicene fragments (MO 214–216, Figure 3a and Figure S13 in the Supporting Information). This observation is also verified for the LUMO and LUMO+1 (MO 217 & 218, Figure 3a), which suggest a reduced impact of the helicenic structures on the rotational strengths associated with the lowest energy excitation and luminescence process. In comparison, the mixed transitions in [7]helicene associated to the lowest energy excitation and luminescence process are well delocalized over the whole helicenic structure (MO 97–103, Figure S6). This qualitative analysis reflects important differences between the multi- and mono-helicenic systems and brings interesting information for the design of more sophisticated chiral polyaromatic compounds with more intense chiroptical properties.

The luminescence properties of both enantiomers C_2-**T7H** were investigated in toluene solution, displaying a broad emission profile with a maximum at 534 nm and a photoluminescence quantum yield (PLQY) of *ca*. 0.04, associated to a fluorescence lifetime of 4 ns (Figure 3c, top). This low PLQY is consistent with the photophysical properties of carbohelicenes and other distorted aromatic systems, which often display significant inter-system crossing efficiency between singlet and triplet excited-states.[22] To gain further insight on this aspect, the emission of C_2-**T7H** was also investigated at 77 K in a frozen 2-MeTHF matrix (see Supporting Information). In these conditions, C_2-**T7H** displays two luminescence responses: a fluorescence emission between 500 and 600 nm, and lower energy signal with a maximum at 694 nm, which was attributed to a phosphorescence process because of the

long lifetime decay on the second timescale, ca. 0.3 s, affording a corresponding T_1 energy level of 1.9 eV (Figure 3c, top). Time-gated emission measurement allowed to isolate the longer-lived phosphorescence emission more specifically (Figure S16 in the Supporting Information), which appears significantly red-shifted in comparison to the classical carbohelicenes ones, suggesting also a delocalisation of the triplet excited-state over more than simply a [7]helicene unit, as in the case of the singlet excited-state S_1. Finally, the two enantiomers of *C*$_2$-**T7H** afforded expected mirror-image circularly polarized luminescence (CPL) spectra in toluene solution (Figure 3c, bottom) with maxima corresponding to those obtained for the unpolarised spectra, and a dissymmetry factor, $|g_{lum}|$, in the magnitude of $2.6 \cdot 10^{-3}$ (at 520–620 nm) as typically observed for organic CPL emitters.[7] Interestingly, the $|g_{lum}|/|g_{abs}|$ ratio is close to 1, indicating that both the ground state and the emitting excited state of *C*$_2$-**T7H** have similar chiral geometries, with few structural and electronic relaxation before the emission process.[23] The absence of possible conformational change has been further confirmed by recording the optical, photophysical and chiroptical properties of the enantiopure compounds in solvents of different polarity. Indeed, similar UV-vis, ECD, fluorescence and CPL responses were obtained in toluene, dichloromethane and acetone (Figures S18–S20 in the Supporting Information), indicating also the absence of charge-transfer character on the low energy transitions, in line with the calculated π-π* frontier molecular orbitals (Figure S13 in the Supporting Information). Finally, the CPL brightness, $\boldsymbol{B}_{CPL}$,[24] of compound *C*$_2$-**T7H** was estimated to be 0.52 $M^{-1} \cdot cm^{-1}$, a modest value in comparison to other organic CPL emitters, mainly because of its low molar extinction coefficient and low emission quantum yield.

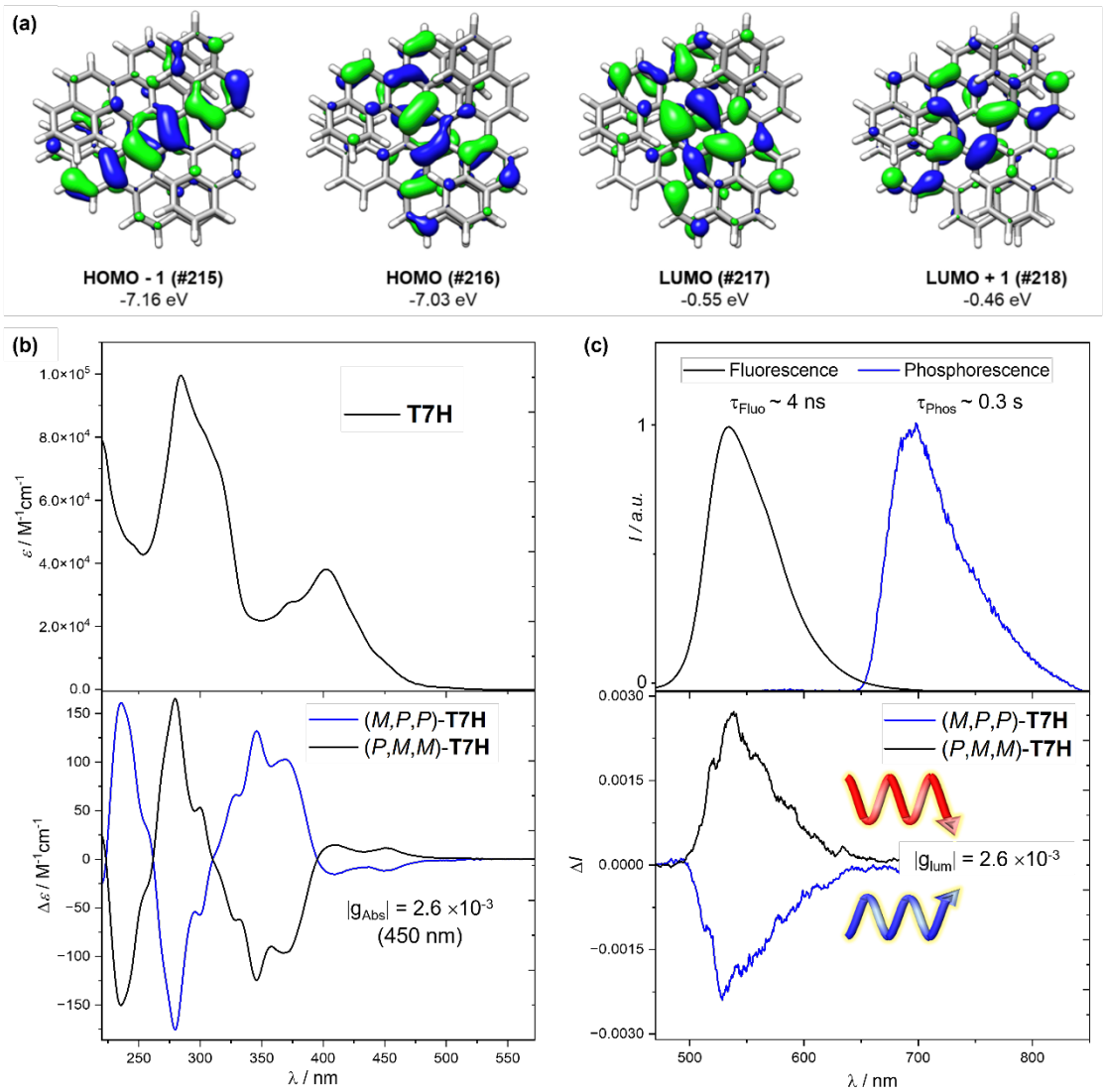

Figure 3. a) Frontier molecular orbitals computed at the ωB97XD/def2TZVP//ωB97XD/def2SVP (gas phase) level of theory with isosurfaces ±0.03 a.u. (blue = negative; green = positive). b) Top: UV-vis spectrum of (*P,M,M*)-C_2-**T7H** in dichloromethane (≈10^{-5} M); bottom: ECD spectra of (*M,P,P*)-**T7H** (blue) and (*P,M,M*)-**T7H** (black) in dichloromethane at 298 K (≈10^{-5} M). c) Top: normalized fluorescence spectrum of (*P,M,M*)-**T7H** (black, solid line) measured in toluene at 298 K (≈10^{-5} M) and its phosphorescence spectrum (blue, solid line) recorded in 2-methyltetrahydrofuran at 77 K, respectively, using a time-gated mode (excitation at 400 nm); bottom: CPL spectra of (*M,P,P*)-**T7H** (blue) and (*P,M,M*)-**T7H** (black) in toluene (≈10^{-5} M) at 298 K.

Conclusions

The enantiomers of an overcrowded triply fused carbo[7]helicene with C_2-symmetry were resolved by semi-preparative HPLC to afford enantiomerically pure samples. Independent recrystallizations of these materials afforded two sets of single-crystals, which allowed to resolve their structures by X-ray diffraction analysis, and to determine their absolute configurations with the highest confidence. In the solid state, the enantiopure and racemate materials showed comparable extreme torsion at the central 'benzene' ring, measured in all three cases at 36.5°. However, the negative curvature of two picene units was found significantly more pronounced in the enantiopure materials, with distal interplanar angles up to 41.4°. The rate constant for the racemization of the overcrowded triply fused carbo[7]helicene could be determined experimentally, thereby providing an experimental measurement of its barrier to enantiomerization $\Delta G_{enant}^{\ddagger}$. The experimentally determined value of $\Delta G_{enant}^{\ddagger}$ was found in excellent agreement with the value of $\Delta G_{enant}^{\ddagger}$ obtained computationally by DFT modeling, with less than 3% deviation, thereby identifying a suitable level of theory to further examine in silico the properties. The photophysical and chiroptical properties, including absorption and emission properties, of the enantiomers of the overcrowded triply fused carbo[7]helicene were examined in detail. Notably, the molecule afforded a green CPL with a $|g_{lum}|$ $2.6 \cdot \times 10^{-3}$ and far-red phosphorescence at low temperature. The similarity between the absorption and luminescence dissymmetry factors $|g|$ indicated that the ground and excited states have similar geometries, and present a significant delocalization on more than a single [7]helicene unit despite the severe contortion of its core six-membered ring.

Experimental Section

See the Supporting Information file.

Associated Content

- Data Availability Statement

The data underlying this study are available in the published article, in its Supporting Information, and openly available in ioChem-BD at http://dx.doi.org/10.19061/iochem-bd-6-285

• Supporting Information (Experimental and computational details on the conformational analysis, the chiral HPLC resolution of the enantiomers, the structural analysis, the kinetic of enantiomerization, and the photophysical and chiroptical properties.)

Acknowledgments

This work was funded by the French Agence Nationale de la Recherche – ANR (ANR-19-CE07-0041). The institutional financial support from the French Ministry of Higher Education, Research and Innovation, Aix-Marseille University, University of Rennes, Centrale Méditerranée and the CNRS is acknowledged. A. A. acknowledges the Spanish Ministerio de Universidades and the EU for a Margarita Salas grant (REQ2021_A_02). We thank the Centre Régional de Compétences en Modélisation Moléculaire (AMU) for computing facilities.

References

(1) Reviews: a) Shen, Y.; Chen, C.-F. Helicenes: Synthesis and Application. *Chem. Rev.* **2012**, *112*, 1463–1535. b) Gingras, M. One hundred years of helicene chemistry. Part 1: non-stereoselective syntheses of carbohelicenes. *Chem. Soc. Rev.* **2013**, *42*, 968–1006. c) Gingras, M.; Félix, G.; Peresutti, R. One hundred years of helicene chemistry. Part 2: stereoselective syntheses and chiral separations of carbohelicenes. *Chem. Soc. Rev.* **2013**, *42*, 1007–1050. d) c) Gingras, M. One hundred years of helicene chemistry. Part 3: applications and properties of carbohelicenes. *Chem. Soc. Rev.* **2013**, *42*, 1051–1095. e) Chen, C.-F.; Shen, Y. Helicene chemistry: From synthesis to applications. Springer Berlin, Heidelberg, 2016. f) Crassous, J.; Stará, I. G.; Starý, I., Eds., Helicenes: Synthesis, Properties and Applications, Wiley-VCH, 1st ed., 2022.

(2) a) Weitzenbeck, R.; Klingler, A. Synthese der isomeren Kohlenwasserstoffe 1, 2-5, 6-Dibenzanthracen und 3, 4-5, 6-Dibenzphenanthren. *Monatsh. Chem.* **1918**, *39*, 315–323. b) Flammand-Barbieux, M.; Nasielski, J.; Martin, R. H. Synthesis of heptahelicene (1): benzo[c]phenanthro[4,3-g]phenanthrene. *Tetrahedron Lett.* **1967**, *7*, 743–744.

(3) a) Carr, R.; Evans, N. H.; Parker, D. Lanthanide complexes as chiral probes exploiting circularly polarized luminescence. *Chem. Soc. Rev.* **2012**, *41*, 7673–7686. b) Han, J. M.; Guo, S.; Lu, H.; Liu, S. J.; Zhao, Q.; Huang, W. Recent Progress on Circularly Polarized Luminescent Materials for Organic Optoelectronic Devices. *Adv. Opt. Mater.* **2018**, *6*, 1800538. c) Kunnen, B.; Macdonald, C.; Doronin, A.; Jacques, A.; Eccles, M.; Meglinski, I. Application of circularly polarized light for non-invasive diagnosis of cancerous tissues and turbid tissue-like scattering media. *J. Biophotnics* **2015**, *8*, 317–323. d) Lindemann, M.; Xu, G.; Pusch, T.; Michalzik, R.; Hofmann, M. R.; Žutić, I.; Gerhardt, N. C. Ultrafast spin-lasers. *Nature* **2019**, *568*, 212–215. e) Novikova, T.; Pierangelo, A.; Manhas, S.; Benali, A.; Validire, P.; Gayet, B.; Martino, A. D. The origins of polarimetric image contrast between healthy and cancerous human colon tissue. *Appl. Phys. Lett.* **2013**, *102*, 241103. f) Wang, H.; liu, L.; Lu, C. CPLC: Visible Light Communication based on Circularly Polarized Light. *Procedia Comput. Sci.* **2018**, *131*, 511–519.

(4) Reviews: a) Dhbaibi, K.; Favereau, L.; Crassous, J. Enantioenriched Helicenes and Helicenoids Containing Main-Group Elements (B, Si, N, P). *Chem. Rev.* **2019**, *119*, 8846–8953. b) Saleh, N.; Shen, C.; Crassous, J. Helicene-based transition metal complexes: synthesis, properties and applications. *Chem. Sci*. **2014**, *5*, 3680–3694. c) Gauthier, E. S.; Rodríguez, R.; Crassous, J. Metal-based multihelicenic architectures. *Angew. Chem. Int. Ed.* **2020**, *59*, 1433–7851.

(5) Reviews: a) Li, C.; Yang, Y.; Miao, Q. Recent Progress in Chemistry of Multiple Helicenes. *Chem. Asian J.* **2018**, *13*, 884–894. b) Kato, K.; Segawa, Y.; Itami, K. Symmetric Multiple Carbohelicenes. *Synlett* **2019**, *30*, 370–377.

(6) Brandt, J. R.; Salerno, F.; Fuchter, M. J. The added value of small-molecule chirality in technological applications. *Nat. Rev. Chem.* **2017**, *1*, 0045.

(7) Mori, T. Chiroptical Properties of Symmetric Double, Triple, and Multiple Helicenes. *Chem. Rev.* **2021**, *121*, 2373−2412.

(8) Clar, E.; Ironside, C. T.; Zander, M. The Electronic Interaction between Benzenoid Rings in Condensed Aromatic Hydrocarbons. 1:12-2:3-4:5-6:7-8:9-10:11-Hexa-benzocoronene,

1:2-3:4-5:6-10:11-Tetrabenzoanthanthrene, and 4:5-6:7-11:12-13:14-Tetrabenzoperopyrene. *J. Chem. Soc.* **1959**, 142–147.

(9) Marom, H.; Pogodin, S.; Agranat, I. Double fjord motif in overcrowded large polycyclic aromatic hydrocarbons: the conformational space of hexabenzo[*a,cd,f,j,lm,o*]perylene. *Polycycl. Aromat. Compd.* **2007**, *27*, 295–310.

(10) Goedicke, C; Stegemeyer, H. Resolution and racemization of pentahelicene. *Tetrahedron Lett.* **1970**, *12*, 937–940.

(11) a) Laarhoven, W. H.; Cuppen, Th. J. H. M. Synthesis of a double helicene, rac. and meso diphenanthro 3,4-c;3'4-1 chrysene. *Tetrahedron Lett.* **1971**, *12*, 163–164. b) Laarhoven, W. H.; Cuppen, Th. J. H. M.; Nivard, R. J. F. Photodehydrocyclizations of stilbene-like compounds-XI: Synthesis and racemization of the double helicene diphenanthro[4.3-a; 3'.4'-o]picene. *Tetrahedron* **1974**, *30*, 3343–3347.

(12) Martin, R. H.; Eyndels, Ch.; Defay, N. Double helicenes: diphenanthro[4,3-a; 3',4'-o]picene and benzo[s]diphenanthro[4,3-a; 3',4'-o]picene. *Tetrahedron* **1974**, *30*, 3339–3342.

(13) a) Barnett, L.; Ho, D. M.; Baldridge, K. K.; Pascal, R. A. The Structure of Hexabenzotriphenylene and the Problem of Overcrowded "D_{3h}" Polycyclic Aromatic Compounds. *J. Am. Chem. Soc.* **1999**, *121*, 727–733. b) Peña, D.; Pérez, D.; Guitián, E.; Castedo, L. Synthesis of Hexabenzotriphenylene and Other Strained Polycyclic Aromatic Hydrocarbons by Palladium-Catalyzed Cyclotrimerization of Arynes. *Org. Lett.* **1999**, *1*, 1555–1557. c) Peña, D.; Cobas, A.; Pérez, D.; Guitián, E.; Castedo, L. Kinetic Control in the Palladium-Catalyzed Synthesis of C_2-Symmetric Hexabenzotriphenylene. A Conformational Study. *Org. Lett.* **2000**, *2*, 1629–1632.

(14) Tanaka, H.; Kato, Y.; Fujiki, M.; Inoue, Y.; Mori, T. Combined Experimental and Theoretical Study on Circular Dichroism and Circularly Polarized Luminescence of Configurationally Robust D_3-Symmetric Triple Pentahelicene. *J. Phys. Chem. A* **2018**, *122*, 7378−7384.

(15) Hu, Y.; Wang, X.-Y.; Peng, P.-X.; Wang, X.-C.; Cao, X.-Y.; Feng, X.; Müllen, K.; Narita, A. Benzo-Fused Double [7]Carbohelicene: Synthesis, Structures, and Physicochemical Properties. *Angew. Chem. Int. Ed.* **2017**, *56*, 3374 –3378.

(16) Martin, R. H.; Marchant, M. J. Thermal racemisation of hepta-, octa-, and nonahelicene. Kinetic results, reaction path and experimental proofs that the racemisation of hexa-

and Heptahelicene does not involve an intramolecular double Diels–Alder reaction. *Tetrahedron* **1974**, *30*, 347–349.

(17) Ferreira, M.; Naulet, G.; Gallardo, H.; Dechambenoit P.; Bock, H.; Durola, F. A Naphtho-Fused Double [7]Helicene from a Maleate-Bridged Chrysene Trimer. *Angew. Chem. Int. Ed.* **2017**, *56*, 3379 –3382.

(18) a) Hosokawa, T.; Takahashi, Y.; Matsushima, T.; Watanabe, S.; Kikkawa, S.; Azumaya, I.; Tsurusaki, A.; Kamikawa, K. Synthesis, Structures, and Properties of Hexapole Helicenes: Assembling Six [5]Helicene Substructures into Highly Twisted Aromatic Systems. *J. Am. Chem. Soc.* **2017**, *139*, 18512−18521. b) Berezhnaia, V.; Roy, M.; Vanthuyne, N.; Villa, M.; Naubron, J.-V.; Rodriguez, J.; Coquerel, Y.; Gingras, M. Chiral Nanographene Propeller Embedding Six Enantiomerically Stable [5]Helicene Units. *J. Am. Chem. Soc.* **2017**, *139*, 18508−18511. c) Zhang, F.; Michail, E.; Saal, F.; Krause, A.-M.; Ravat, P. Stereospecific Synthesis and Photophysical Properties of Propeller-Shaped $C_{90}H_{48}$ PAH. *Chem. Eur. J.* **2019**, *25*, 16241–16245. d) Roy, M.; Berezhnaia, V.; Villa, M.; Vanthuyne, N.; Giorgi, M.; Naubron, J.-V.; Poyer, S.; Monnier, V.; Charles, L.; Carissan, Y.; Hagebaum-Reignier, D.; Rodriguez, J.; Gingras, M.; Coquerel, Y. Stereoselective Syntheses, Structures, and Properties of Extremely Distorted Chiral Nanographenes Embedding Hextuple Helicenes. *Angew. Chem. Int. Ed.* **2020**, *59*, 3264–3271.

(19) Artigas, A.; Rigoulet, F.; Giorgi, M.; Hagebaum-Reignier, D.; Carissan, Y.; Coquerel, Y. Overcrowded Triply Fused Carbo[7]helicene. *J. Am. Chem. Soc.* **2023**, *145*, 15084−15087.

(20) a) Shibata, K.; Kulkarni, A. A.; Ho, D. M.; Pascal, R. A. Perchlorotriphenylene. *J. Am. Chem. Soc.* **1994**, *116*, 5983−5984. b) Shibata, K.; Kulkarni, A. A.; Ho, D. M.; Pascal, R. A. The Pursuit of Perchlorotriphenylene. *J. Org. Chem.* **1995**, *60*, 428–434. c) Hursthouse, M. B.; Smith, V. B.; Massey, A. G. The crystal and molecular structure of dodecafluorotriphenylene, $C_{18}F_{12}$. *J. Fluor. Chem.* **1977**, *10*, 145–155.

(21) Nakai, Y.; Mori, T.; Inoue, Y. Theoretical and Experimental Studies on Circular Dichroism of Carbo[n]helicenes. *J. Phys. Chem. A* **2012**, *116*, 7372−7385.

(22) a) Sapir, M.; Vander Donckt, E. Intersystem crossing in the helicenes. *Chem. Phys. Lett.* **1975**, *36*, 108–110. b) Nijegorodov, N. I.; Downey, W. S. The Influence of Planarity and Rigidity on the Absorption and Fluorescence Parameters and Intersystem Crossing Rate Constant in Aromatic Molecules. *J. Phys. Chem.* **1994**, *98*, 5639–5643. c) Nagarajan, K.;

Mallia, A. R.; Muraleedharan, K.; Hariharan, M. Enhanced intersystem crossing in core-twisted aromatics. *Chem. Sci.* **2017**, *8*, 1776–1782.

(23) Cei, M.; Di Bari, L.; Zinna, F. Circularly polarized luminescence of helicenes: A data-informed insight. *Chirality* **2023**, *35*, 192–210.

(24) L. Arrico, L. Di Bari, F. Zinna Quantifying the Overall Efficiency of Circularly Polarized Emitters. *Chem. Eur. J.* **2021**, *27*, 2920–2934.